Construction of Green Nanostructured Heterogeneous Catalysts via Non-Covalent Surface Decoration of Multi-Walled Carbon Nanotubes with Pd(II) Complexes of Azamacrocycles

Matteo Savastano,[a] Paloma Arranz-Mascarós,[b] Carla Bazzicalupi,[a] Maria Paz Clares,[c] Maria Luz Godino-Salido,[b] Maria Dolores Gutíerrez-Valero,[b] Mario Inclán,[c] Antonio Bianchi,[a*] Enrique García-España[c*] and Rafael Lopez-Garzón[b*]

[a] Department of Chemistry "Ugo Schiff", University of Florence, Italy. E-mail antonio.bianchi@unifi.it

[b] Department of Inorganic and Organic Chemistry, University of Jaén, Spain. E-mail rlopez@ujaen.es

[c] Institute of Molecular Sciences, University of Valencia, Spain. E-mail

Abstract

Green nanostructured heterogeneous catalysts were prepared via a bottom up strategy. Designed ligands were synthesized joining covalently an electrondeficient pyrimidine residue and a scorpiand azamacrocycle. The desired molecular properties were easily transferred to nanostructured materials in two steps: first, exploiting their spontaneous chemisorption onto multi-walled carbon nanotubes (MWCNTs) via the pyrimidinic moiety in water at room temperature, then, taking advantage of the easy coordination of Pd(II) to the azamacrocycle in the same conditions. An evenly distribution of catalytic centres was obtained on the MWCNTs surface. Catalytic properties of these materials were assessed towards the Cu-free Sonogashira cross coupling, leading to significant improvements in terms of yields and reaction conditions, especially when considering the possibility to maintain yields of 90%, or above, in a feasible amount of time (2h), while working under green conditions (water, 50 °C, aerobic atmosphere). The catalysts proved to be reusable for several cycles with good yields.

Keywords: palladium(II) catalysis, Sonogashira cross coupling, multi-walled carbon nanotubes, azamacrocycles, hybrid materials, non-covalent functionalization.

1. Introduction

Palladium-catalysed coupling reactions, leading to C-C, C-N and C-O bond formation, are highly significant to efficiently access products which would otherwise require far more impractical routes. The advantages they offer are relevant both in terms of costs (yields, reaction rates) and of required synthetic efforts (reaction conditions, selectivity) [1].

Although many of such processes have been developed employing homogeneous catalysts [1,2,3], successive research focused on the development of heterogeneous Pd-catalysts as a more practical solution, on a large scale, capable of overcoming the difficulties in recovering, and thus reusing, expensive homogeneous catalysts, which were moreover found as residuals in the final products. Several substrates have been proposed as possible solid supports, among which many carbon-based materials [4-8].

Carbon nanotubes (CNTs) have gathered a lot of attention in recent years due to their peculiar chemical and physical properties, which makes them suitable for catalytic processes [4,9]. Their non-covalent functionalization has become a topic of interest, as such approach offers not only an effective way to keep composite systems together, but also preserves CNTs unique electronic properties, otherwise widely disrupted through a covalent procedure [9]. Van der Waals forces, especially π-π stacking interactions, have been exploited to decorate CNTs with a variety of species, including nanoparticles [10,11], polymers [12-15], cyclodextrins [16,17], glycolipids [18,19] and biomolecules [20-24]. Porphyrins and phtalocyanines, among other candidates [25-31], have become the ligands of choice for inserting metal cations in such non-covalent assemblies, as they combine their ability to form stable complexes with an aromatic nature, thus giving rise to robust adducts [32-39].

In this paper, we use non-covalent π-π stacking interactions to functionalize commercial MWCNTs with two tetraazamacrocyclic ligands (Scheme 1): the macrocyclic functionalities were used to further decorate the obtained hybrid materials (MWCNT/HL1 and MWCNT/HL2, Fig.1) with Pd(II) and the resulting compounds (MWCNT/HL1-Pd(II) and MWCNT/HL2-Pd(II)) were tested as heterogeneous catalysts for the Sonogashira cross coupling.

As some of us recently showed, pyrimidine residues can be employed as anchor groups for the non-covalent functionalization of activated carbon (AC), thanks to their ability to form strong π-π stacking interactions with the arene centres of such substrate [40]. In particular, the 6-amino-3,4-dihydro-3-methyl-5-nitroso-4-oxopyrimidine group has proved particularly efficient to this purpose, as it allowed the irreversible attachment of several ligands of the Ar-S-F type (Scheme 2) on AC to obtain hybrid materials that were employed

for the extraction of both metal cations [41-44] and anionic species [45,46] from aqueous media.

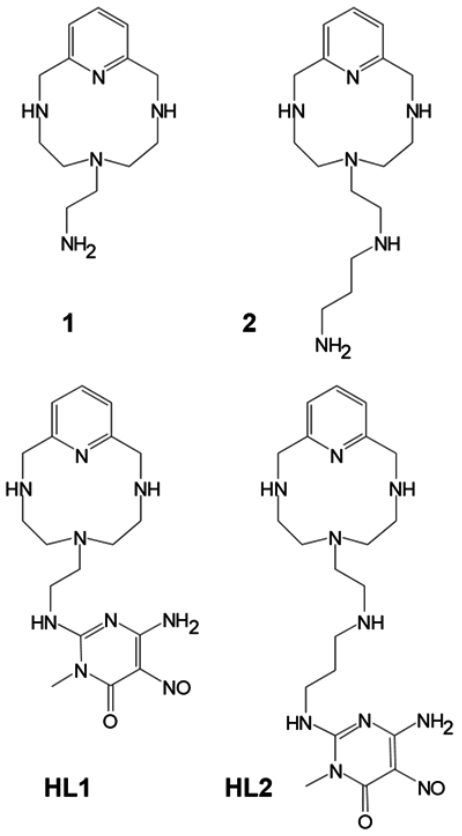

Scheme 1. The ligands HL1 and HL2 along with their precursor molecules **1** and **2**.

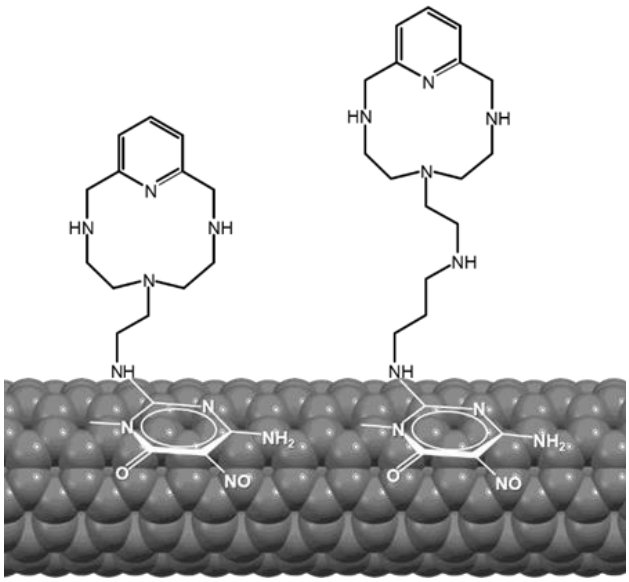

Fig. 1. Schematic representation of the non-covalent functionalization of a MWCNT with HL1 and HL2 to provide MWCNT/HL1 and MWCNT/HL2, respectively.

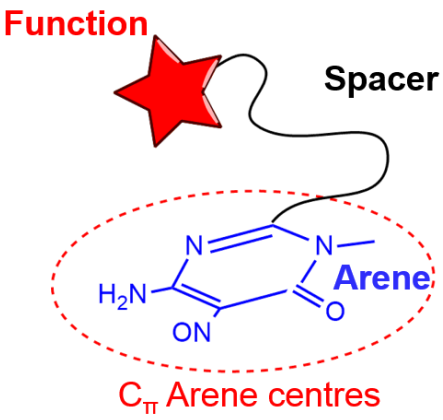

Scheme 2. General structure of an Ar-S-F ligand.

Furthermore, in a recent work [47], some of us assessed the catalytic properties of three AC-supported Pd-catalysts, prepared by the same route, towards the hydrogenation of 1-octene, demonstrating how the enhancement in the conversion efficiency and reaction times are due to the preparation method itself.

The whole body of gathered experimental evidences, which guided us in the design of the new heterogeneous catalysts herein reported, points out several strong points of our approach. First, convenience and simplicity: with a proper choice of the anchoring group, the grafting process takes place spontaneously when CNTs are suspended in an aqueous solution of the ligand at room temperature [40-47]; the same can be said for the coordination of metal cations [41-44] to the macrocyclic moiety of the grafted ligands, thermodynamics driving the system together effortlessly in such conditions. Second, the self-assembly of our systems not only allows a high degree of control over the chemical nature and amount of catalytic sites, but also ensures their homogeneous distribution on the supporting substrate [47].

The higher uniformity of the catalysts produced by the above route correlates well with their observed superior overall performances over other published systems. Such correlation stands out even more if one considers that many reported catalysts are prepared through direct deposition of Pd-nanoparticles (potentially more heterogeneous in size and nature than a molecular active site and surely harder to spread evenly on a surface), without assisting ligands or with ligands covalently linked to the substrate, often requiring pre-emptive surface modification [4].

In view of the previous remarks, also the choice of CNTs as supporting material can be fully explained: not only the chosen functionalization method is able to preserve their peculiar properties [4,9], but they stand out as a quasi-molecular material. Compared to AC, CNTs possess less defects and chemical functionalities and a wholly exposed surface area,

lacking micropores that may limit the diffusion of reagents to the active sites, or trap the reaction products causing the poisoning of the catalyst over time [47].

The copper-free Sonogashira coupling has been chosen as catalytic test. Such reaction has been largely conducted under homogeneous conditions in the presence of phosphine-palladium catalysts, $Pd(PPh_3)_4$ and $PdCl_2(PPh_3)_2$ being the most commonly used, although many other candidates have been explored, including palladium complexes with bidentate phosphines and polydentate ligands bearing nitrogen and oxygen donors [48]. The air sensitivity of phosphine ligands, which demands the use of an inert atmosphere, and the difficulty to recycle such homogeneous catalysts have hindered their large-scale application. Heterogeneous catalysts have attracted considerable interest, in the last years, as convenient alternatives to overcome such drawbacks, addressing the recovery of the catalyst by means of simple separation methods [48]. Several supporting materials have been proposed, such as silica [49-51], polymers [52-56], ionic liquids [52,57-60], metal organic frameworks (MOFs) [61,62] and CNTs [4,9,63-70], for the immobilization of metal (mostly palladium) complexes or metal nanoparticles [52,71-75].

Successfully, our heterogeneous MWCNT/HL1-Pd and MWCNT/HL2-Pd catalysts, herein reported, proved efficient in promoting the Sonogashira coupling between phenylacetylene and iodobenzene to give diphenylacetylene in water under aerobic conditions in almost quantitative yields, even at low temperatures. They are easily recoverable and reusable with appreciable conservation of their efficacy for at least four catalytic cycles. Accordingly, this type of catalysts, their preparation method and their application conditions are very promising to define new protocols for environmentally and economically sustainable carbon-carbon bond-making processes.

2. Experimental

2.1. Synthesis of HL1and HL2

0.38 g (1,52 mmol) of 6-(2-aminoethyl)-3,6,9-triaza-1-(2,6)-pyridinecyclodecaphane [76] (**1**) dissolved in 20 cm^3 of methanol were reacted at room temperature with 0.35 g (1.73 mmol) of 6-amino-3,4-dihydro-3-methyl-2-methoxy-5-nitroso-4-oxopyrimidine [77]. The latter dissolves slowly over 8 h under stirring. The excess of pyrimidine was then converted into the insoluble 2,4-diamino-1-methyl-5-nitroso-6-oxopyrimidine derivative by reaction with ammonia (5 drops of 37% aqueous ammonia). After standing overnight in a fridge, the resulting suspension was filtered and the solution was evaporated to dryness under vacuum

at room temperature to obtain HL1 as a deep purple solid compound. Yield 95%. $C_{18.5}H_{31}N_9O_{3.5}$ (HL1·0.5MeOH·H_2O): calcd. C 51.02, H 7.18, N 28.94; found C 50.93, H 7.19, N 28.70. ^{1}H NMR D_2O: δ (ppm) 2.62-3.46 (m, 13H), 3.74 (t, 2H), 4.55 (s, 4H), 7.37 (d, 2H), 7.88 (t, 1H).

HL2 was prepared by reaction of 6-(7-amino-3-azahexyl)-3,6,9-triaza-1-(2,6)-pyridinecyclodecaphane [78] (**2**) with 6-amino-3,4-dihydro-3-methyl-2-methoxy-5-nitroso-4-oxopyrimidine according to the procedure adopted for the synthesis of HL1. Yield 73%. $C_{22}H_{37}N_{10}O_4$ (HL2·MeOH·H_2O): calcd. C 51.95, H 7.93, N 27.53; found C 52.30, H 7.68, N 27.68. ^{1}H NMR D_2O: δ (ppm) 2.90-3.28 (m, 15H), 3.34 (s, 3H), 3.66 (t, 2H), 4.56 (s, 4H), 7.38 (d, 2H), 7.88 (t, 1H).

2.2. Potentiometric measurements

Potentiometric (pH-metric) titrations, employed to determine the protonation constants of the studied ligands and of their Pd(II) complexes, were performed in 0.1 M NMe_4Cl at 298.1±0.1 K using an automated apparatus and a procedure previously described [79]. The combined Metrohm 6.0262.100 electrode was calibrated as an hydrogen-ion concentration probe by titration of previously standardized amounts of HCl with CO_2-free NaOH solutions and determining the equivalent point by Gran's method [80], which gives the standard potential, $E°$, and the ionic product of water (pK_w = 13.83(1) in 0.1 M NMe_4Cl at 298.1 K). The computer program HYPERQUAD [81] was used to calculate the stability constants from the potentiometric data. The concentration of ligands was about 1×10^{-3} M in all experiments. The studied pH range was 2.0-11.5. At least two measurements were performed for each system: at first, the different titration curves were treated as separated curves without significant variations in the values of the calculated stability constants; finally, the sets of data were merged together and treated simultaneously to give the final stability constants. Although it was not possible to determine the equilibrium constants for the formation of PdL^+ complexes with both ligands due to the slowness of the complexation reactions, these species proved to be very stable once formed and could be titrated in the pH range 2.5-11.5 according to fast protonation equilibria. Titrations were performed by means of the above method onto solutions containing L (L = HL1, HL2) and K_2PdCl_4 (1×10^{-3} M) equilibrated for 10 days at pH 3 and 298 K, thus making possible the determination of the complexes protonation constants. Different equilibrium models for the studied systems were generated by eliminating and introducing different species. Only those models for which the

HYPERQUAD program furnished a variance of the residuals $\sigma^2 \leq 9$ were considered acceptable. Such condition was unambiguously met by a single model for each system.

2.3. Spectroscopic measurements

Absorption spectra were recorded at 298 K on a Jasco V-670 spectrophotometer. Both ligand and metal complex solutions were about 5×10^{-5} M. ^{1}H NMR spectra (400 MHz) in D_2O solution were recorded at 298 K on a 400 MHz Bruker Avance III spectrometer. XPS spectra were obtained in a Kratos Axis Ultra DLD spectrometer. Monochromatic Al/MgKα radiation from twin anode in constant analyser energy mode with pass energy of 160 and 20 eV (for the survey and high resolution spectra, respectively) was used. The C1s transition at 284.6 eV was used as a reference to obtain the heteroatoms binding energies. The accuracy of the binding energy (BE) values was ±0.2 eV.

2.4. Adsorption studies

The equilibrium time for the adsorption of HL1 and HL2 on CNTs was determined experimentally by kinetic measurements. The data points were obtained by mixing 0.0250 g of the adsorbent with 25 mL of a 10^{-3} M aqueous solution of the adsorbate at a given initial pH value. The obtained suspension was kept at 298.1 K under continuous shaking while concentration of the adsorbate was regularly monitored by checking its UV-absorbance at the isosbestic point, 302 nm in the case of HL1 and 304 nm in the case of HL2, until the equilibrium (3 days) was reached.

The adsorption isotherms were obtained under the same conditions (298.1 K, 0.0250 g of adsorbent suspended in 25 mL of the appropriate solution of the adsorbate at the chosen pH value). The ligand concentration values ranged from 8×10^{-5} M to 2×10^{-3} M. The samples were shaken in a thermostatic air-incubator until the determined equilibrium time was reached. Desorption isotherms of the ligands from the MWCNT/HL1 and MWCNT/HL2 hybrid materials were obtained point-by-point from the adsorption isotherms, recovering, drying, weighting and re-suspending the solid in water, maintaining a 1 mg of material/1 mL water ratio, then following a similar procedure to that described for the adsorption isotherms.

2.5. Determination of the surface charge density of MWCNT/HL1 and MWCNT/HL2

The surface charge density (Q in mmol H^+/g of adsorbent) of both materials was determined by a method based on potentiometric titration data [82,83], following an already

described procedure [46]. Q was calculated by means of the equation $Q = \frac{1}{m}(V_0 + V_t)([H]_i - [OH]_i - [H]_e + [OH]_e)$, where V_0 and V_t are the volumes of initial solution and titrant, respectively, and m is the mass of the adsorbent. Subscripts i and e refer to the initial and equilibrium concentration of protons or hydroxyl ions. The proton isotherms are obtained by plotting Q vs equilibrium pHs.

2.6. Preparation of the catalysts

The two catalysts, MWCNT/HL1-Pd and MWCNT/HL2-Pd, were prepared following a two-step procedure. First, we prepared MWCNT/HL1 and MWCNT/HL2 materials, adsorbing the ligands on commercial CNTs (Thin MWCNTs Nanocyl, Ref 3100, Spain, with metal oxides content ≤ 5%). This was accomplished according to the following procedure for both ligands: 0.5 g of the adsorbent were mixed with 500 mL of 10^{-3} M aqueous solution of the ligand at pH = 7.5 in a plastic flask. This pH value was proved to be the optimum for the highest irreversible loading of the ligand. The flask was shaken in an air-thermostated bath at 298.1 K until the adsorption equilibrium was reached (3 days). The obtained solids, MWCNT/HL1 and MWCNT/HL2, were separated by filtration, washed repeatedly with distilled water and dried into a desiccator. The final amount of adsorbent per gram of adsorbate was quantified in 0.36 mmol of HL1 and 0.31 mmol of HL2 per g of CNT, respectively.

In the second step, MWCNT/HL1-Pd and MWCNT/HL2-Pd catalysts were prepared by coordination of Pd(II), as K_2PdCl_4, on the appropriate CNT/ligand material. Accordingly, 0.5 g of the corresponding CNT/ligand material were mixed in a suitable plastic flask with 500 mL of a 1 M KCl aqueous solution containing K_2PdCl_4 5×10^{-4} M, whose pH had been adjusted to 5.0 through HCl addition. pH 5.0 was selected as the best compromise between the minimization of proton competition towards the coordination of Pd(II) with the amino groups of the ligands and the avoidance of the formation of Pd(II) hydroxy-species, that, at this pH value, are not yet formed (i.e. all the Pd(II) is present as $[PdCl_4]^{2-}$) [84]. The suspensions were shaken in an air-thermostated bath at 298.1 K within four days until the adsorption equilibrium was reached (i.e. when the UV absorbance of the Pd(II) solution at λ=474 nm remained constant over time). Finally, the amount of adsorbed Pd(II) was determined as the difference between the initial and final absorbances at λ=474 nm: 0.45 mmol Pd per gram of CNT/HL1 and 0.40 mmol per gram of CNT/HL2 were assessed.

2.7. General procedure for the Sonogashira reaction

A mixture of iodobenzene (1 mmol), phenylacetylene (1 mmol), Et_3N (2 mmol), H_2O (1 mL) and the catalyst (22 mg of MWCNT/HL1-Pd or 25 mg of MWCNT/HL2-Pd, relationship reactants/Pd(II) = 100) was stirred under aerobic conditions at a constant temperature (30, 50 or 70 °C). The progress of the reaction was monitored by gas chromatography (GC). After completion, $CHCl_3$ (10 mL) was added to the reaction mixture and the catalyst was recovered by filtration and washed with $CHCl_3$ (2 x 5 mL) and H_2O (2 x 5 mL). The aqueous and organic layers were separated through a separatory funnel. The organic layer was dried over anhydrous $MgSO_4$. The analysis of the reaction products in the organic phase was performed by GC using a 7820A Agilent GC System chromatograph, with an Agilent 190915-433 column, 30 m × 250 µm × 25 µm and a flame ionization detector (FID). The recovered catalyst was reused for another batch of the same reaction. The process was repeated for three additional runs.

3. Results and discussion

3.1. Acid-base properties of HL1 and HL2

Potentiometric (pH-metric) titrations performed in aqueous solution (0.1 M Me_4NCl, 298.1 K) in the pH range 2.0-11.5 showed that HL1 and HL2 contain, respectively, four and five basic groups undergoing protonation, as well as an acidic group that starts being deprotonated above pH 10. The equilibrium constants determined for these processes are reported in Table 1 in the form of protonation constants. Distribution diagrams of the protonated species formed as a function of pH are reported as supplementary materials (Fig.S1).

According to the properties of other amine derivatives with the same pyrimidine residue, the protonation stages occurring at the highest pH values (log*K* = 11.13, 11.21, Table 1) should involve the amine groups directly connected to the pyrimidine ring, which are expected to be deprotonated at high pH, while the protonation stages corresponding to the log*K* values of 2.3 and 2.2 (Table 1) should involve the pyrimidine nitroso groups. This assignment of the protonation sites is confirmed by the pH dependence of the adsorption spectra of both ligands.

As shown in Fig.2 for HL1 and in Fig.S2 for HL2, the near-UV spectra are characterized by three bands centered at about 230, 265 and 330 nm corresponding to allowed π/π^* transitions between π-orbitals of the pyrimidinic group and overlapping with the band at about 265 nm of the pyridinic one. The spectra of both HL1 and HL2 display a marked pH

dependence in acidic and alkaline solution, when protonation involves the pyrimidine chromophore, while in the intermediate pH region (4.0-9.0 approximately) they are almost invariant since protonation takes place on the non-chromogenic aliphatic amine groups.

Table 1. Protonation constants of ligands HL1 and HL2 (L) in 0.1 M NMe_4Cl at 298.1±0.1 K.

Equilibria	**log*K***	
	HL1	**HL2**
$L^- + H^+ = HL$	11.13(4)[a]	11.21(5)
$HL + H^+ = H_2L^+$	9.28(5)	9.71(4)
$H_2L^+ + H^+ = H_3L^{2+}$	7.83(7)	8.64(6)
$H_3L^{2+} + H^+ = H_4L^{3+}$	2.3(1)	7.51(6)
$H_4L^{3+} + H^+ = H_5L^{4+}$	1.6(5)	2.2(1)
$H_5L^{4+} + H^+ = H_6L^{5+}$		1.6(5)

[a] Values in parentheses are standard deviation on the last significant figures.

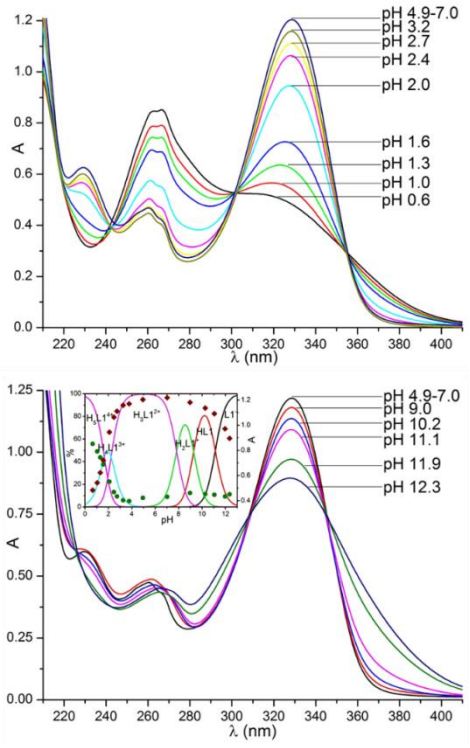

Fig. 2. UV absorption spectra of HL1 at different pH in aqueous solution: pH 0.6-7.0 (top), pH 4.9-12.3 (bottom). Inset (bottom): pH dependence of the 330 nm (red diamonds) and 265 nm (green dots) absorbances.

Interestingly, the equilibrium constants for the protonation stages involving the chromophores of the two ligands are equal, or almost equal, within the experimental errors, in agreement with protonation occurring on almost identical sites, while, for the remaining proton binding processes, HL2 demonstrates a greater basicity, in terms of values and number of the protonation constants, according to the presence of one more amine group in its structure. The highly protonated H_5L1^{4+} and H_6L2^{6+} species are formed only in small amounts in the lower pH region we have investigated (Fig.S1). Nevertheless, the discovery of their formation reveals that three out of the four nitrogen atoms of the macrocyclic ring of both ligands can undergo protonation in the studied pH range.

3.2. Formation of Pd(II) complexes in solution

The complexation of Pd(II) by the two ligands HL1 and HL2 takes place very slowly, however, once such complexes are formed, their protonation can be studied without kinetic problems above pH 2.5. Accordingly, we were able to determine the protonation constants for these complexes, shown in Table 2, by means of potentiometric (pH-metric) titration in aqueous solution (0.1 M Me_4NCl, 298.1 K). Distribution diagrams concerning these equilibria can be found in the supplementary materials (Fig.S3).

$[PdL1]^+$ and $[PdL2]^+$ are involved in two and three protonation steps, respectively. The equilibrium constants corresponding to log$K$ = 9.46 and log$K$ = 10.19 for $[PdL1]^+$ and $[PdL2]^+$, respectively, are too high to be associated with protonation of metal-coordinated amine groups while they can be assigned to protonation of metal-free deprotonated amine groups, in agreement with the UV spectral variations observed for these complexes in the alkaline zone (Fig.S4). UV spectra also show that, in the acidic region, protonation corresponding to the smallest equilibrium constants (log$K$ = 2.2 and 2.5, Table 2) occurs on the pyrimidine group. In the case of $[PdL2]^+$, there is an intermediate protonation step (log$K$ = 7.0) corresponding to protonation of the additional amine group in the chain connecting the macrocycle and the pyrimidine moieties of HL2, which is expected not to be coordinated, as the basicity of this amine group in the complex is relatively close to that of the same group in the free ligand (log$K$ = 8.64, Table 1).

An interesting point regards the number of donor atoms used by HL1 and HL2 to bind Pd(II). In the case of the Cu(II) complexes, crystal structures of the $[CuL]^{2+}$ complexes of the precursor molecules 1 ad 2 (Scheme 1) show that the metal is coordinated to all four nitrogen atoms of the macrocycle and to all the nitrogen atoms of the pending arm [76,78]. The crystal structures of the $[ML]^{2+}$ (M = Mn(II), Ni(II), Zn(II)) complexes of L2 are

isostructural to $[CuL2]^{2+}$ [85,86]. In all these structures the macrocycle adopts a folded conformation. As observed above, in the case of the square planar Pd(II) complexes it seems that there is no participation of donor atoms of the appended chains in metal coordination, thus, if the macrocyclic ring of the ligand would assume the expected folded conformation, only three out of the four macrocyclic nitrogen atoms would be coordinated to Pd(II) (Fig.3).

Table 2. Protonation constants of the $[LPd]^{+}$ complexes formed by HL1 and HL2 in 0.1 M NMe_4Cl at 298.1±0.1 K.

Equilibria	**log*K***	
HL =	**HL1**	**HL2**
$[PdL]^{+} + H^{+} = [PdHL]^{2+}$	9.46(6)	10.19(7)
$[PdHL]^{2+} + H^{+} = [PdH_2L]^{3+}$	2.2(2)	7.0(1)
$[PdH_2L]^{3+} + H^{+} = [PdH_3L]^{4+}$		2.5(2)

[a] Values in parentheses are standard deviation on the last significant figures.

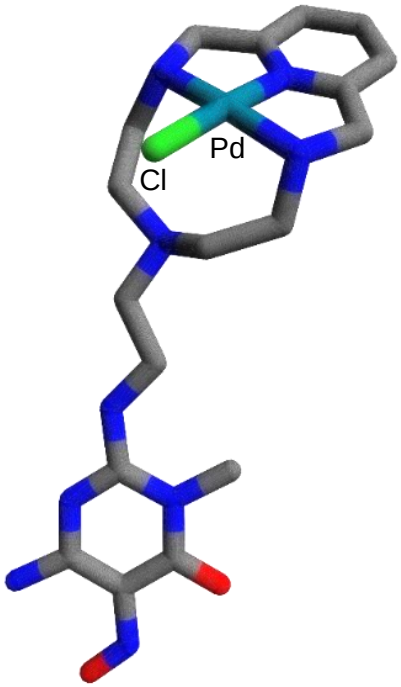

Fig. 3. Outline of the proposed coordination mode for Pd(II) to HL1.

To get information on this point, solutions containing equimolar quantities of ligand and $[PdCl_4]^{2-}$ were equilibrated at pH 4 and 298 K within ten days, for both HL1 and HL2. The UV-Vis spectra of the mixtures were monitored daily: no variations were observed after four

days. The concentration of free Cl^- was then determined by means of ion chromatography evidencing that only three chloride anions were released by $[PdCl_4]^{2-}$ upon coordination. Accordingly, we must assume that in these complexes Pd(II) is coordinated to three macrocyclic nitrogen atoms and one Cl^- anion, as sketched out in Fig.3 for the case of HL1.

3.3. Characterization of the Catalysts

The data on the bare graphitic support are sketched below: for a detailed analysis of the properties of the employed MWCNTs the reader is addressed to a previous paper [87]. The used MWCNTs have C as the main constituent (~96.0 %), H (~0.3%) and little oxygen content as the only heteroatomic component (~3.6%). Negligible amounts of various metal oxides residues, such as chromium, nickel and cobalt, are also presents [88].

The adsorption-desorption isotherms of N_2, determined at 77 K, on MWCNT/HL1-Pd and MWCNT/HL2-Pd, together with the one for the bare MWCNT, appear in Fig.S5. Although little N_2 adsorptions are observed at very low pressures, as in type I isotherms, they are of no account, indicating that the microporosity of the material is irrelevant [88]. Instead, a strong increasing adsorption prevails with a hysteresis loop at high relative pressures, which is typical of type II isotherms, indicating the existence of meso- and macropores with wide distribution sizes, which is consistent with the aggregation of CNTs in bundles. The BET external surface area (determined by applying the BET equation to the N_2 adsorption data) associated to the wide pores of the pristine CNTs, 221 m^2/g, decreases upon adsorption of the ligands, to 198 m^2/g in the case of HL1 and 188 m^2/g in the HL2. These data are consistent with the adsorption of the ligands by π-π interactions of their pyrimidine residues with the arene centres of the external surface of the CNTs [42,43]. Despite the slightly smaller molar amount of adsorbed HL2 per gram of CNTs (0.31 mmol/g) compared to HL1 (0.36 mmol/g), the larger molecular size of the former determines the observed lower BET surface area of MWCNT/HL2 in respect to MWCNT/HL1.

The adsorption and desorption isotherms of HL1 and HL2 on CNTs at pH 4.0 and 7.5 can be found in the supplementary materials (Fig.S6): the manifest high irreversibility of the adsorption processes indicates strong ligand-CNT surface interaction. All adsorption isotherms fit the type 1 of the Giles classification [89], indicating a predominant adsorption mechanism. One can also see how the adsorption capacity of CNTs increases slightly with pH for both ligands: this is due to the number of protonated groups in the polyaminic chains attached to the pyrimidine, which decrease, along with the strength of the ligand-solvent interaction, as the pH increases. These features are consistent with the adsorption of the

ligands by π-π interactions between the heterocyclic moiety of the ligands and the arene centres, C_π, at the CNT surface as previously observed for analogous ligands on graphitized ACs [90].

Profile of surface charge density Q (mmol(H^+)/g) versus pH are reported in Fig.S7 for both functionalized materials, MWCNT/HL1 and MWCNT/HL2, and pristine MWCNTs. Applying the SAIEUS method [91] the respective pKa versus pH profiles were obtained. The plot obtained for pristine CNTs is consistent with the existence of carboxyl groups (pKa ≈ 3) and weakly acidic phenol, lactone and anhydride functions (pKa ≈ 9-10) [92]. Furthermore, the peak at pKa ≈ 6.5 is due to the protonation of the arene centres of the CNTs surface [45,46]. Concerning the hybrid materials, the Q vs pH plots already show how their positive surface charge densities are higher than that of the bare CNTs in a wide pH range (3~10), due to the protonation of the polyamine functions of the anchored ligands. The pKa *vs* pH profiles of MWCNT/HL1 and MWCNT/HL2 (Fig.S7), approximately investigated in the 3.0-10.5 pH range, show no signs of the protonation of C(5)-NO groups of the pyrimidine moieties of the adsorbed ligands (log*K* 2.3 and 2.2 for the free ligands HL1 and HL2, respectively, see Table 1): such evidences suggest that the protonation of those sites is probably hindered due to π-π interactions. Concerning the other protonation steps of the polyamine moieties of the adsorbed ligands, they take place at substantially lower pH values than those observed for the free molecules in solution, indicating a decreasing of the overall basicity of such moieties (cf. Table 1 and Fig.S7). This can probably be rationalized in terms of different conformation of the ligands in solution and at CNTs surface, where an elongated arrangement is required to optimize the stacking interactions, thus hampering to some extent the protonation of such groups.

The XPS spectra of the ligands in the N1s region (Fig.S8) consist of a main peak at about 397.0 eV, pertaining to the aliphatic nitrogen atoms, with shoulders (398.1 eV and 397.5 eV for HL1 and HL2 respectively) relating to the aromatic nitrogen atoms. After adsorption of the ligands on CNTs surface, both components of the N1s signal shift to higher binding energy values (Fig.S8). In the case of the aromatic components, referring to both the pyridine and pyrimidine rings, the shift may indicate a strong plane-to-plane Cπ-pyrimidine interaction, the interacting sites being compressed one onto the other resulting in local repulsion of the adjoined π clouds of both moieties, thus deshielding the N atoms of the pyrimidine. This hypothesis is reinforced by the observation of similar shifts in the binding energies of the C and O atoms of the pyrimidinic ring. These effects are similar to those previously observed with other analogous ligands when adsorbed on graphitized ACs

[42,43] and CNTs (Fig.S9). The shift of the aliphatic N atoms, together with the pyridinic component of the aromatic ones, indicates a change in their chemical environments due to the adsorption process, suggesting changes in the protonation degree of such moieties.

After adsorption of $[PdCl_4]^{2-}$ on the hybrid materials, the binding energy values of the aromatic subunits are almost unmodified, whereas those of the aliphatic moieties increase from 399.6 eV to 400.6 eV for MWCNT/HL1 and from 399.7 eV to 400.6 eV for MWCNT/HL2 (Fig.S8). This points out that Pd(II) ions are complexed by the polyaminic portions of the adsorbed ligands, the increased deshielding of the aliphatic nitrogen atoms being due to the coordination of the metal cations.

Concerning the oxidation state of Pd, XPS spectra of MWCNT/HL1-Pd and MWCNT/HL2-Pd (Fig.4) show two signals in the Pd3d region (343,5 and 338,2 eV) which are characteristics of Pd(II), discarding any reduction to Pd(0).

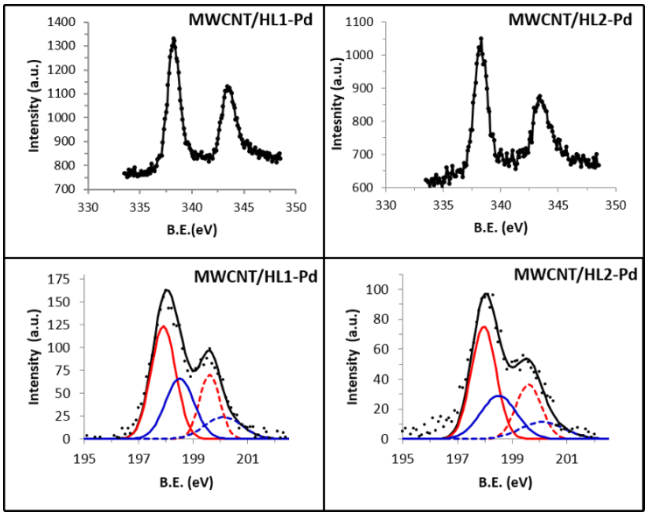

Fig. 4. High resolution XPS spectra of the catalysts useful for the assessment of the nature of the anchored Pd-complex species: top, spectra in the Pd $3d_{5/2}$ and Pd $3d_{3/2}$ regions, bottom, spectra in the Cl $2p_{3/2}$ and Cl $2p_{1/2}$ regions, showing the deconvolution of the twofold peaks into distinct signals.

As the molar amounts of adsorbed Pd(II) are always close to those of adsorbed ligand, for both HL1 and HL2, it is safe to conclude that most, if not all, $[PdCl_4]^{2-}$ is adsorbed via complexation of the palladium ion to the polyamine moieties of the ligands. Inspection of Cl/Pd molar ratio, from Pd and Cl signals of the XPS spectra of both catalysts (Fig.4), reveals that such ratio is invariably very close to 2, reinforcing the idea that the metal is bound to the ligand. Moreover, further insight into the nature of the formed complex could be gained by close inspection of Cl XPS spectra. The two peaks at 198,0 and 199,6 eV, assigned to electrons from $2p_{3/2}$ and $2p_{1/2}$ states respectively, both possess a shoulder peak of

higher energy (198,5 and 200,1 eV severally) (Fig.4); the twofold nature of such peaks correlates with the presence of two distinct chloride anions: the first bound to Pd(II) ions, acting as its fourth donor, the latter being retained upon complexation of Pd(II) to guarantee charge neutrality. This, corroborated by the evidences from the coordination behavior observed in the solution studies of the free ligands, proofs that both HL1 and HL2, adsorbed on CNTs or not, function as N-tridentate ligands towards Pd (II), leading to complexes with an activated position occupied by a chloride anion.

The values of the BET surface areas of the functionalized materials reveal changes in the conformations of the polyaminic chains upon Pd(II) complexation. In the case of MWCNT/HL1, the BET surface area diminishes significantly after the coordination of the metal (from 198m^2/g of the precursor to 179m^2/g), while for MWCNT/HL2 there is barely a detectable difference (from 188 to 183 m^2/g). This can be rationalized considering the tendency of the formed square-planar Pd(II) complexes to interact with CNTs surface by Cπ-dπ interactions, which should result in a decrease of the BET surface area. Such interaction justifies both the data for HL1 and HL2: for the first ligand, the required folding of the polyaminic chain is not hindered, resulting in the interaction of the Pd(II)-macrocycle complex with the graphitic surface which actively reduces the surface area; in the case of HL2, the possible formation of such interactions is thought to be hindered both by the electrostatic interaction with the additional ammonium group in the side chain, which in Pd(II) adsorption conditions (pH 5.0) is expected to be protonated (log*K*=7.0 for the free complex, see Table 2), and by the higher loss of conformational entropy of the chain required to establish Cπ-dπ contacts compared to the shorter HL1. Thus, in this latter case, the variation of the BET surface area upon Pd(II) complexation is found to be very modest.

3.4. The Sonogashira carbon-carbon coupling reaction

The catalytic activity of MWCNT/HL1–Pd and MWCNT/HL2–Pd materials towards the copper-free Sonogashira reaction between iodobenzene and phenylacetylene (1:1 molar relationship) using water as solvent and triethylamine as base was tested at three different temperatures (see Table 3).

At 30 °C, the reaction was not completed until 3 days. This high reaction time could be attributed to the extreme insolubility of the reactants in water, preventing their diffusion to the polar active-centres. Then, the reaction was assayed at 50 °C. At this temperature, although the solubility of the reactants in water is still poor, probably acting as a limiting

Table 3. Catalytic assays of the two catalysts towards the Cu-free Sonogashira coupling between iodobenzene and phenylacetylene (1 mmol of each, 1 ml H_2O, Et_3N 2 mmol, 1% mol Pd).

Catalyst	T(°C)	Cycle	Time	Yield (%)
MWCNT/HL1-Pd	30	1	3 d	88
	50	1	2 h	90
		2	8 h	86
		3	8 h	80
		4	24 h	80
	70	1	2 h	84
MWCNT/HL2-Pd	30	1	3 d	87
	50	1	2 h	94
		2	16 h	92
		3	24 h	76
		4	24 h	66
	70[a]		2 h	83

[a] At this temperature desorption of the anchored HL2-Pd complex was observed.

kinetic factor, the C-C coupling reaction was completed in 2 hours: 90% of conversion of the reactants into diphenyl acetylene was achieved in the case of MWCNT/HL1-Pd and 94% for MWCNT/HL2-Pd, moreover without formation of any other by-product. The calculated TOF values (mmol of reactants/mmol Pd(II)-amino complexes transformed per second) were 0.021 s^{-1} and 0.024 s^{-1} for MWCNT/HL1-Pd and MWCNT/HL2-Pd, respectively. The shortened equilibrium times, even at lower temperature, than most proposed Pd(II)-based heterogeneous catalysts, (see Table 4) along with the high yields obtained, are probably due to the easy accessibility of the catalytic active centres, reinforced by their homogeneous dispersion over the whole external surface of the CNTs.

It should also be mentioned that, after recovering the catalysts by simple filtration methods and washing them with chloroform and water, their XPS spectra still showed traces of adsorbed iodobenzene. This points out that the partial adsorption of iodobenzene on the CNTs surface likely prevents that 100% conversion is reached in both cases.

To explore the influence of higher temperatures on the coupling, tests were also carried out at 70 °C. In the case of MWCNT/HL2-Pd catalyst, a significant lixiviation of the anchored complex was observed which becomes evident as a pink colouring appears in the aqueous phase: as a consequence, an unsatisfactory yield was obtained. Nevertheless, this should be regarded as an important result, since such behavior demonstrates the heterogeneous nature of the catalyst, as an increased desorption of the Pd-HL2 complex not

only does not improve the yield, but lowers it. In the case of MWCNT/HL1-Pd, containing the smaller and less protonated HL1, no lixiviation was noticed, but neither the yields (84% of diphenylacetylene formed) nor the equilibrium time (2 hours) improved from the 50°C assay.

The studied C-C coupling reaction, was also carried out i) without any catalyst, ii) with the MWCNTs used as support of the catalysts, iii) with MWCNT/HL1 and MWCNT/HL2, but no reaction was observed in any of such cases. In addition, the catalytic activity of a MWCNT/$[PdCl_4]^{2-}$ material, consisting of $[PdCl_4]^{2-}$ directly adsorbed on CNTs, was assessed at 50 °C. In this case, the C-C coupling reaction did take place, with an equilibrium time of 24 hours, after which a 78% of conversion of the reactants in diphenylacetylene was reached.

Table 4. Catalytic performances of MWCNT/HL1-Pd and MWCNT/HL2-Pd and selected carbon-based catalysts assessed for Cu-free Sonogashira Coupling.

Catalyst/ Support	Pd %[a]	T (°C)	Time (h)	Base	Solvent[b]	Molar ratio[c]	Atmosphere	Yield (%)	Ref
Pd(II)-HL1 complex/ MWCNT	1	50	2	Et_3N	H_2O (1 mL)	1:1:2	Aerobic	90	[d]
Pd(II)-HL2 complex/ MWCNT	1	50	2	Et_3N	H_2O (1 mL)	1:1:2	Aerobic	94	[d]
Pd(II)-Schiff base complex/MWCNT	1.2	27 55 90	24 6 1	Et_3N	H_2O (2 mL)	1:1.5:2	Aerobic	64 81 95	68
Pd(0) NPs/ pramipexole-MWCNT	0.1 0.1	80 80	2 12	Et_3N K_2CO_3	DMF (3 mL) H_2O (3 mL)	1:1.2:2 1:1.2:2	Unspecified	96 55	93
Electrodeposited Pd(0) NPs/ MWCNT	1	Reflux	2.5	K_2CO_3	MeOH/H_2O (3mL:1mL)	1:1.2:1.5	Aerobic	71	94
Pd(0) NPs/ Iminopyridine-MWCNT	1	120	0.5	K_2CO_3	DMF (4 mL)	1:1:1	Unspecified	98	65
Pd(0) NPs/ Nanoporous CHT	0.23	80	10-18	Cs_2CO_3	DMF (5 mL)	1:1.5:1.5	Inert	85	95

[a] 100(mol Pd/mol reagent); [b] mL solvent/mmol Iodobenzene; [c] Iodobenzene: Phenylacetylene:Base; [d] This study.

3.5. Reusability of the catalysts

The reusability of the two heterogeneous catalysts was tested for the above Sonogashira coupling reaction under the same conditions: three additional runs were carried out after the

first one. After each cycle the catalysts were separated by filtration, washed thoroughly with chloroform and water and dried before reusing. As one can see in Table 3, the catalysts maintain a good catalytic activity through the four reaction cycles. In the second reaction cycle the yields of the reactions are close to those of the first run. For MWCNT/HL1-Pd catalyst, the yield decreases to 80% in the third cycle, value which is maintained in the fourth reaction. In the case of MWCNT/HL2-Pd, a higher decrease of the catalytic activity is observed after the second reaction, as the yields start to decrease with each cycle. Parallel to the above, a significant increase of the equilibrium times was observed for both catalysts after the first run, this effect being again sharper for MWCNT/HL2-Pd than for MWCNT/HL1-Pd.

To get insight into the possible causes of this behavior, the catalysts were characterized after each cycle to detect any possible modification occurring under their repeated use. The elemental analyses of the catalysts reveal nitrogen losses with each use, obviously involving the corresponding ligands HL1 and HL2, which are more substantial for MWCNT/HL2-Pd than for MWCNT/HL1-Pd (Table S1). Such decreasing is sharper in the earliest cycles, after which the nitrogen content almost remains stable. It should be noted how the catalytic activities of the material decreases in parallel with the nitrogen losses they suffer. Very scarce amounts of Pd(0) nanoparticles were observed in the TEM images of reused MWCNT/HL1-Pd catalyst, while none could be found in the case of MWCNT/HL2-Pd (Fig.5): this might be due to the superior stability of HL2-Pd complexes or to the different number of donor atoms in the ligands. According to the proposed mechanism for the copper-free Sonogashira reaction, the presence of Pd(0) should be related to the formation of a Pd(0) complex as an intermediate species during the catalyzed process [48]. Nevertheless, the XPS spectra of the materials in the Pd region, collected after each cycle (Fig.S10), show signals at similar values than in the fresh catalysts, *i.e.* 343.5 and 338.2 eV, discarding the reduction of Pd(II) to Pd(0) as a possible cause of the deactivation of the catalysts, which seems better to be related to nitrogen losses. Furthermore, the ratio between the intensities of N1s and Pd3d signals in the XPS spectra of reused catalysts remains similar to that of the fresh ones. This clearly suggests that the deactivation of the catalysts is due to the lixiviation of the anchored HL1-Pd and HL2-Pd complexes during the reactions. The mechanism of loss of catalytic centres, however, appears different from what some of us previously observed in the case of hydrogenation reactions with AC-supported Pd(II) amino complexes [47], where pyrimidine residues stuck to the graphitic walls while the appended chain was partially lost due to solvolysis of the $C(2)_{Pyrimidine}$-NH bond. In those cases, the solvolysis

was thought to be promoted by the stereochemical restrictions suffered by molecules adsorbed in the micropores of the carbon support. The lack of microporosity in our CNTs-based systems, along with the steady N/Pd ratio observed, lead to the conclusion that the partial lixiviation of catalytic centres observed in this study should be attributed to the competition of the hydrophobic molecules (phenylbenzene, iodobenzene and phenylacetylene) with the adsorbed HL1-Pd and HL2-Pd complexes for the C_π centers of the CNT surface.

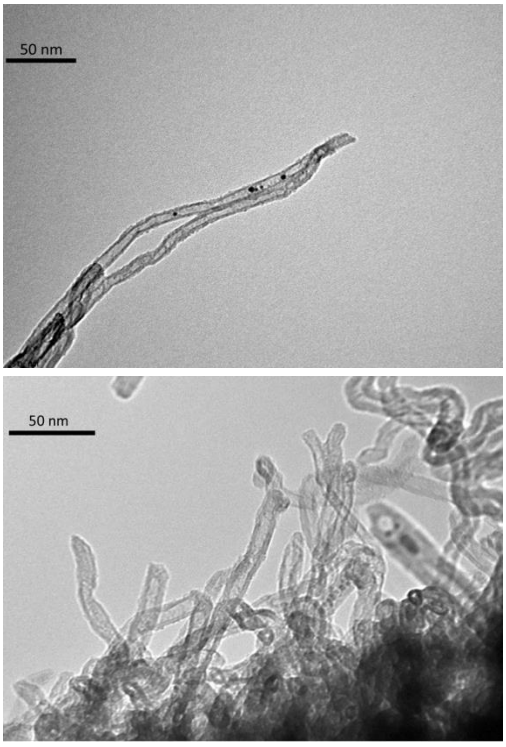

Fig. 5. TEM Images of MWCNT/HL1-Pd 4th cycle (top) and MWCNT/HL2-Pd 4th cycle (bottom).

4. Conclusions

The gathered experimental evidences strongly support the assayed MWCNT/HL1-Pd and MWCNT/HL2-Pd materials as valuable catalysts for the Cu-free Sonogashira coupling reaction: as one can easily see comparing the obtained results with other candidates (Table 4), our systems not only rank among the first in terms of yields and reaction times, but the conditions (solvent and temperature) in which they are capable of such performances are unprecedented; such finding deserves to be underlined, especially in an era striving for green, sustainable and energy-saving chemical processes. Accordingly, also the choices of a carbonaceous support and of a single Pd(II) ion as catalytic active site should be stressed as

environmentally friendly solutions, adding to the convincing heterogeneous nature of our catalysts.

As documented above, the strong points underlying their striking catalytic activity reside in the uniformity of the catalytic sites, both in terms of surface distribution and chemical environment, which is granted by the preparation method.

Another feature worth mentioning is the choice of the polyaminic ligands, which are not only capable of coordinating Pd(II) strongly, forming a macrocyclic complex which is mostly stable under re-use even under stern alkaline conditions, but also manage to maintain an activated position, occupied by a chloride anion in the free complex and in the fresh catalyst, in the metal's first coordination sphere, which is probably crucial for the observed catalytic activity.

These promising results encourage the extension of this research to ligands possessing more than one pyrimidine moiety to ensure a firmer sorption and improve the overall re-usability of these materials, while maintaining the observed high catalytic performances.

Acknowledgements

Financial support from the following institutions is gratefully acknowledged: MIUR (project 2015MP34H3), Spanish MICINN and MEC and FEDER funds from the European Union (grants CTQ2013-14892 and CTQ2016-78499-C6-1-R), Unidad de Excelencia María de Maeztu MDM-15-0538), Generalitat Valenciana (PROMETEO II 2015-002), MINECO (Project MAT2014-60104-C2-2-R) and the Autonomous Regional Government Junta de Andalucía (Group PAIDI FQM273).

Appendix A. Supplementary materials

Supplementary data associated with this article can be found, in the online version, at

References

[1] C.C.C. Johansson Seechurn, M.O. Kitching, T.J. Colacot, V. Snieckus, Angew. Chem. Int. Ed. 51 (2012) 5062–5085.

[2] "The Nobel Prize in Chemistry 2010 - Advanced Infor-mation". Nobelprize.org. Nobel Media AB 2014. Web. 13 Dec 2016. <http://www.nobelprize.org/nobel_prizes/chemistry/laureates/2010/advanced.html>

[3] S.A. Timofeeva, M.A. Kinzhalov, E.A. Valishina, K.V. Luzyanin, V.P. Boyarskiy, T.M. Buslaeva, M. Haukka, V.Y. Kukushkin, J. Catal. 329 (2015) 449–456.

[4] P. Serp, B. Machado, Nanostructured Carbon Materials for Catalysis, RSC Catalysis Series No. 23, The Royal Society of Chemistry, Cambridge, 2015, pp. 370–375.
[5] L. Yin, J. Liebscher, Chem. Rev. 107 (2007) 133–173.
[6] A. Fihri, M. Bouhrara, B. Nekoueishahraki, J.-M. Basset, V. Polshettiwar, Chem. Soc. Rev. 40 (2011) 5181–5203.
[7] J. Guerra, M.A. Herrero, Nanoscale 2 (2010) 1390-1400.
[8] Q. Zhao, Y. Zhu, Z. Sun, Y. Li, G. Zhang, F. Zhang, X. Fan, J. Mater. Chem. A 3 (2015) 2609-2616.
[9] W. Maser, A.M. Benito, E. Muñoz, M.T. Martinez, in: A. Vaseashta, I.N. Mihailescu (Eds.), Functionalized Nanoscale Materials, Devices and Systems, Springer, Dordrecht, The Netherlands, 2008, pp. 101−119.
[10] T.A. Saleh, V.K. Gupta, in: A. Tiwari, S.K. Shukla (Eds.), Advanced Carbon Materials and Technology, Wiley Online Library, 2014, pp. 317–330.
[11] L. Hu, Y.-L. Zhao, K. Ryu, C. Zhou, J. F. Stoddart, G. Grüner, Adv. Mater. 20 (2008) 939−946.
[12] T. Fujigaya, N. Nakashima, Sci. Tech. Adv. Mat. 16 (2015) 1−21.
[13] P. Bilalis, D. Katsigiannopoulos, A. Avgeropoulos, G. Sakellariou, RSC Adv. 4 (2014) 2911–2934.
[14] D. Tuncel, Nanoscale 3 (2011) 3545-3554.
[15] D. Ravelli, D. Merli, E. Quartarone, A. Profumo, P. Mustarelli, M. Fagnoni, RSC Adv. 3, (2013) 13569–13582.
[16] G. Zhu, X. Zhang, P. Gai, X. Zhang, J. Chen, Nanoscale 4 (2012) 5703–5709.
[17] Y.-L. Zhao, L. Hu, J. F. Stoddart, G. Grüner, Adv. Mater. 20 (2008) 1910−1915.
[18] M. Assali, M.P. Leal, I. Fernandez, N. Khiar, Nanotechnology 24 (2013) 085604/1–085604/12.
[19] M. Assali, M.P. Leal, I. Fernandez, R. Baati, C. Mioskowski, N. Khiar, Soft Matter. 5 (2009) 948−950.
[20] S. Marchesan, M. Prato, Chem. Commun. 51 (2015) 4347–4359.
[21] P. Yadav, V. Rastogi, A.K. Mishra, A. Verma, Drug Deliv. Lett. 4 (2014) 156–169.
[22] A. Battigelli, C. Menard-Moyon, T. Da Ros, M. Prato, A. Bianco, Adv. Drug Deliv. Rev. 65 (2013) 1899-1920.
[23] G. Lamanna, A. Battigelli, C. Menard-Moyon, A. Bianco, Nanotechnol. Rev. 1 (2012) 17-29.

[24] S.K. Vashist, D. Zheng, G. Pastorin, K. Al-Rubeaan, J. H. T. Luong, F. S. Sheu, Carbon 49 (2011) 4077–4097.
[25] B.I.K. Kharisov, O.V. Kharissova, J. Coord. Chem. 67 (2014) 3769–3808.
[26] S.F. Liu, S. Lin, T.M. Swager, ACS Sens. 1 (2016) 354–357.
[27] C.C. Gheorghiu, C. Salinas-Martinez de Lecea, M. C. Roman-Martinez, Appl. Cat. A 478 (2014) 194–203.
[28] P. Gou, N.D. Kraut, I.M. Feigel, A. Star, Macromolecules 46 (2013) 1376–1383.
[29] V.A. Basiuk, L.V. Henao-Holguin, E. Alvarez-Zauco, M. Bassiouk, E.V. Basiuk, Appl. Surf. Sci. 270 (2013) 634–647.
[30] E.V. Basiuk, E.V. Rybak-Akimova, V.A. Basiuk, D. Acosta-Najarro, J. M. Saniger, Nano Lett. 2 (2002) 1249–1252.
[31] V.A. Basiuk, J. Phys. Chem. B 108 (2004) 19990–19994.
[32] G. Bottari, O. Trukhina, M. Ince, T. Torres, Coord. Chem. Rev. 256 (2012) 2453–2477.
[33] F. D'Souza, O. Ito, Chem. Soc. Rev. 41 (2012) 86–96.
[34] F. Vialla, G. Delport, Y. Chas-Sagneux, Ph. Roussignol, J.S. Lauret, C. Voisin, Nanoscale 8 (2016) 2326–2332.
[35] S.F. Liu, L.C.H. Moh, T.M. Swager, Chem. Mater. 27 (2015) 3560–3563.
[36] E. Ma-ligaspe, A.S.D. Sandanayaka, T. Hasobe, O. Ito, F. D'Souza, J. Am. Chem. Soc. 132 (2010) 8158–8164.
[37] T. Hasobe, S. Fukuzumi, P. V. Kamat, J. Am. Chem. Soc. 127 (2005) 11884–11885.
[38] B. Wang, X. Zhou, Y. Wu, Z. Chen, C. He, Sensor. Actuat. B-Chem. 171-172 (2012) 398–404.
[39] A. Satake, Y. Miyajima, Y. Kobuke, Chem. Mater. 17 (2005) 716–724.
[40] R. López-Garzón, M.L. Godino-Salido, M.D. Gutíerrez-Valero, P. Arranz-Mascarós, M. Melguizo, C. García, M. Domingo-García, F.J. López-Garzón, Inorg. Chim. Acta 417 (2014) 208–221.
[41] J. García-Martín, M.L. Godino-Salido, R. López-Garzón, M.D. Gutiérrez-Valero, P. Arranz-Mascarós, H. Stoeckli-Evans, Eur. J. Inorg. Chem. (2008) 1095–1106.
[42] M.D. Gutiérrez-Valero, M.L. Godino-Salido, P. Arranz-Mascarós, R. López-Garzón, R. Cuesta, J. García-Martín, Langmuir 23 (2007) 5995–6003.
[43] J. García-Martín, R. López-Garzón, M.L. Godino-Salido, M.D. Gutiérrez-Valero, P. Arranz-Mascarós, R. Cuesta, F. Carrasco-Marín, Langmuir 21 (2005) 6908–6914.

[44] J. García-Martín, R. López-Garzón, M. L. Godino-Salido, R. Cuesta-Martos, M.D. Gutiérrez-Valero, P. Arranz-Mascarós, H. Stoeckli-Evans, Eur. J. Inorg. Chem. (2005) 3093–3103.
[45] M. Savastano, P. Arranz-Mascarós, C. Bazzicalupi, A. Bianchi, C. Giorgi, M.L. Godino-Salido, M.D. Gutiérrez-Valero, R. López-Garzón, RSC Adv. 4 (2014) 58505–58513.
[46] P. Arranz, A. Bianchi, R. Cuesta, C. Giorgi, M.L. Godino, M.D. Gutiérrez, R. López, A. Santiago, Inorg. Chem. 49 (2010) 9321–9332.
[47] M.L Godino-Salido, M.D. Gutiérrez-Valero, R. López-Garzón, P. Arranz-Mascarós, A. Santiago-Medina, M. Melguizo, M. Domingo-García, F.J. López-Garzón, V.K. Abdelkader-Fernández, C. Salinas-Martínez de Lecea, M. C. Román-Martínez, RSC Adv. 6 (2016) 58247–58259.
[48] R. Chinchilla, C. Nájera, Chem. Soc. Rev. 40 (2011) 5084–5121.
[49] M. Opanasenko, P. Stepnicka, J. Cejka, RSC Adv. 4 (2014) 65137–65162.
[50] V. Polshettiwar, C. Len, A. Fihri, Coord. Chem. Rev. 253 (2009) 2599-2626.
[51] R.B. Bedford, U.G., Singh, R.I. Walton, R.T. Williams, S.A. Davis, Chem. Mater. 17 (2005) 701–707.
[52] A. Kumbhar, R. Salunkhe, Curr. Org. Chem. 19 (2015) 2075–2121.
[53] C.G. Frost, L. Mutton, Green Chem. 12 (2010) 1687–1703.
[54] M. Bakherad, S. Jajarmi, J. Mol. Catal. A-Chem. 370 (2013) 152–159.
[55] A. Alonso, A. Shafir, J. Mascanás, A. Vallribera, M. Muñoz, D.N. Muraviev, Catal. Today 193 (2012) 200–206.
[56] Z.J. Wang, S. Ghasimi, K. Landfester, K.A.I. Zhang, Chem. Mater. 27 (2015) 1921–1924.
[57] R. Munirathinam, J. Huskens, W.Verboom, Adv. Synth. Catal. 357 (2015) 1093–1123.
[58] J.C. Hierso, M. Beauperin, S. Saleh, A. Job, J. Andrieu, M. Picquet, C. R. Chim. 16 (2013) 580–596.
[59] T. Miao, L. Wang, P.H. Li, J.C. Yan, Synthesis (2008) 3828–3834.
[60] C.K. Lee, H.H. Peng, I.J.B. Lin, Chem. Mater. 16 (2004) 530–536.
[61] C.I. Ezugwu, B. Mousavi, M.A. Asraf, Z. Luo, F. Verpoort, J. Catal. 344 (2016) 445–454.
[62] J. Huang, W. Wang, H. Li, ACS Catal. 3 (2013) 1526–1536.
[63] J. John, E. Gravel, I.N.N. Namboothiri, E. Doris, Nanotechnol. Rev. 1 (2012) 515–539.
[64] J. Guerra, M.A. Herrero, Nanoscale 2 (2010) 1390–1400.

[65] H. Veisi, M. Adib, R. Karimi-Nami, New J. Chem. 40 (2016) 4945-4951.
[66] A. Ohtaka, J.M. Sansano, C. Najera, I. Miguel-Garcia, A. Berenguer-Murcia, D. Cazorla-Amoros, ChemCatChem 7 (2015) 1841–1847.
[67] C. Rossy, J. Majimel, Tréguer M. Delapierre, E. Fouquet, F.-X. Felpin, Appl. Catal. A-Gen. 482 (2014) 157–162.
[68] M. Navidi, N. Rezaei, B. Mo-vassegh, J. Organomet. Chem. 743 (2013) 63–69.
[69] J. Jin, Z. Dong, J. He, R. Li, J. Ma, Nanoscale Res. Lett. 4 (2009) 578–583.
[70] M. Salavati-Niasari, M. Bazarganipour, Appl. Surf. Sci. 255 (2009) 7610–7617.
[71] A.J. Reay, I.J.S. Fairlamb, Chem. Commun. 51 (2015) 16289–16307.
[72] M.O. Sydnes, Curr. Org. Chem. 18 (2014) 312–326.
[73] A. Ohtaka, Chem. Rec. 13 (2013) 274–285.
[74] A. Balanta, C. Godard, C. Claver, Chem. Soc. Rev. 40 (2011) 4973–4985.
[75] B. Karimi, H. Behzadnia, E. Farhangi, E. Jafari, A. Zamani, Curr. Org. Synth. 7 (2010) 543-567.
[76] B. Verdejo, A. Ferrer, S. Blasco, C.E. Castillo, J. González, J. Latorre, M.A. Máñez, M. García Basallote, C. Soriano, E. García-España, Inorg. Chem. 46 (2007) 5707–5719.
[77] N.J. Low, M.D. López, P. Arranz, J. Cobo, M.L. Godino, R. López, M.D. Gutiérrez, M. Melguizo, G. Ferguson, C. Glidewell, Acta Cryst. B 56 (2000) 882–892.
[78] M. Inclán, M.T. Albelda, J.C. Frías, S. Blasco, B. Verdejo, C. Serena, C. Salat-Canela, M.L. Díaz, A. García-España, E. García-España, J. Am. Chem. Soc. 134 (2012) 9644–9656.
[79] C. Bazzicalupi, A. Bianchi, C. Giorgi, P. Gratteri, P. Mariani, B. Valtancoli, Inorg. Chem. 52 (2013) 2125–2137.
[80] G. Gran, Analyst (London) 77 (1952) 661–671.
[81] P. Gans, A. Sabatini, A. Vacca, Talanta 43 (1996) 1739–1753.
[82] T.J. Bandosz, J. Jagiello, C. Contescu, J.A. Schwarz, Carbon, 31 (1993) 1193–1202.
[83] J. Jagiello, T.J. Bandosz, J.A. Schwarz, Carbon 32 (1994) 1026–1028.
[84] C.F. Baes, R.E. Mesmer, *The Hydrolysis of Cations*, John Wiley and Sons, New York, 1976.
[85] M.P. Clares, C. Serena, S. Blasco, A. Nebot, L. del Castillo, C. Soriano, A. Domènech, A.V. Sánchez-Sánchez, L. Soler-Calero, J.L. Mullor, A. García-España, E. García-España, J. Inorg. Biochem. 143 (2015) 1–8.
[86] S. Blasco, *Complejos Metálicos de Compuestos Poliaminicos y su Aplicación como Miméticos de Enzimas Protec-toras Antioxidantes*, Ph. D. Thesis, University of Valencia, 2011.

[87] F. Morales-Lara, M.J. Perez-Mendoza, D. Altmajer-Vaz, M. García-Roman, M. Melguizo, F.J. Lopez-Garzón, M. Domingo-García, J. Phys. Chem. C 117 (2013) 11647−11655.

[88] V.K. Abdelkader-Fernández, *Hyperbranched structures on carbon nanotubes to obtain supported metal nanoparticles: attachment by means of halogenated functions and direct functionalization*, Ph. D. Thesis, University of Granada (Spain), 2015.

[89] C.H. Giles, T.H. MacEwan, S.N. Nakhwa, D.Smith, *J. Chem. Soc.*, 1960, 3973–3993.

[90] R. López-Garzón, M.L. Godino-Salido, M.D. Gutiérrez-Valero, P. Arranz-Mascarós, M. Melguizo, C. García, M. Domingo-García, F.J. López-Garzón. Inorg. Chim. Acta 417 (2014) 208-221.

[91] J. Jagiello, T. Bandosz, K. Putyera, J. Schwarz, J. Colloid Interface Sci. 172 (1995) 341–346.

[92] M.L. Godino-Salido, R. López-Garzón, M.D. Gutiérrez-Valero, P. Arranz-Mascarós, M. Melguizo-Guijarro, M.D. López de la Torre, V. Gómez-Serrano, M. Alexandre-Franco, D. Lozano-Castelló, D. Cazorla-Amorós, M. Domingo-García, Mat. Chem. Phys. 143 (2014) 1489–1499.

[93] S. Abbasi, M. Hekmati, Appl. Organomet. Chem. DOI: 10.1002/aoc.3600.

[94] M. Radtke, S. Stumpf, B. Schröter, S. Höppener, U. S. Schu-bertb, A. Ignaszak, Tetrahedron Lett. 56 (2015) 4084–4087.

[95] A. Modak, A. Bhaumik, J. Mol. Catal. A-Chem. 425 (2016) 147–156.